European Review for Medical and Pharmacological Sciences 2020; 24: 74-85

# Long non-coding RNA BLACAT1 inhibits prostate cancer cell proliferation through sponging miR-361

H.-Y. LI[1], F.-Q. JIANG[1], L. CHU[2], X. WEI[1]

[1]Department of Urology, China-Japan Union Hospital of Jilin University, Changchun, People's Republic of China
[2]Department of Bidding and Purchase, China-Japan Union Hospital of Jilin University, Changchun, People's Republic of China

**Abstract. – OBJECTIVE: LncRNAs play a key role in the development and progression of prostate cancer. In this study, the effects of the lncRNA BLACAT1 in prostate cancer were investigated.**

**PATIENTS AND METHODS: Real-time PCR was used to detect the expression of BLACAT1 and miR-361 in prostate cancer tissues and adjacent normal tissues (n=25). The function of BLACAT1 was detected through proliferation assay and apoptosis assay. The interaction between BLACAT1 and miR-361 in prostate cancer was studied by luciferase assay, RNA immunoprecipitation assay and chromatin immunoprecipitation analysis were performed to detect the BLACAT1 binding proteins. The xenograft mice experiment was performed to further confirm the functional significance of lncRNA BLACAT1 *in vivo*.**

**RESULTS: In patient samples and prostate cancer cell lines, BLACAT1 was down-regulated and inversely proportional to DNMT1, HDAC1, EZH2, MDM2 and miR-361 expression. Treatment with 5-azacytidine and chidamide enhanced *BLACAT1* expression and decreased the levels of miR-361. The BALCAT1 promoter was methylated in prostate cancer tissue and found to interact with miR-361 via luciferase assays. BLACAT1 bound to EZH2, DNMT1 and HDAC1. ChIP-seq analysis revealed that HDAC1 interacts with STAT3, while EZH2 interacts with the mitogen-activated protein kinase (MAPK) promoter.**

**CONCLUSIONS: Two regulatory axes of BLACAT1-EZH2-MAPK and BLACAT1-HDAC1-STAT3 were identified to be associated with the progression of prostate cancer. Both chidamide and 5-azacytidine represent promising therapeutic options in prostate cancer treatment.**

*Key Words:*
Prostate cancer, 5-azacytidine, Chidamide, EZH2, HDAC1.

## Introduction

Globally, prostate cancer remains a leading cause of mortality[1,2]. Prostate cancer is the 3rd most common cancer across the world, and it typically affects males aged over 55 years[3]. The lack of early symptoms makes prostate cancer diagnosis challenging[4]. Magnetic resonance imaging (MRI) is the most effective way to identify prostate cancer, with detection rates of 85-100%. Prostate specific antigen (PSA) is a protein produced in the prostate gland, elevated levels of which can be suggestive of prostate cancer. In the clinic, elevated PSA levels frequently lead to unnecessary biopsies. Despite intense research efforts, the mechanisms of prostate cancer development remain poorly characterized[5] and effective therapeutic treatment regimens are lacking.

Long non-coding RNAs (lncRNAs) are frequently dysregulated in an array of cancers[6] including prostate cancer[7]. For example, *HCG11* is poorly expressed in prostate cancer cells and associated with poor survival in afflicted patients[8]. Previous studies revealed that the expression of prostate cancer associated lncRNA transcript 1 (PCAT-1) inhibits cell proliferation through miR-145-5p sponging[9]. LncRNA bladder cancer associated transcript 1 (*BLACAT1)* was firstly found in bladder cancer[10], and the silencing of BLACAT1 prevents tumor growth and promotes cancer cell death[11]. Conversely in colorectal cancer, *BLACAT1* expression is suppressed, highlighting its differential effects according to cancer tissue/status[12]. In prostate cancer cells, the cellular roles of BLACAT1 and its potential involvement in prostate cancer development have not been defined.

As a form of small non-coding RNAs, microRNAs (miRNAs) target specific cellular mRNA sequences to either suppress or sustain



*Corresponding Author:* Xin Wei, MD; e-mail: weinxin@jlu.edu.cn

the expression of cellular genes[13]. MiR-361 shows pro-oncogenic effects in a range of human cancers. Competing endogenous RNAs (ceRNA) act as sponges that upregulate or downregulate target miRNAs. The roles of miR-361 in prostate cancer cells and its interaction with lncRNAs have not been defined.

Epigenetics represents the study of heritable alterations in gene copy numbers in the absence of genetic mutations[14]. DNA methylation has emerged as a critical driver of tumor development, most thoroughly characterized in nasopharyngeal carcinoma[15]. The methylation of LncRNAs has gained intense interest in cancer genetics through the identification of its ability to regulate the expression of epithelial splicing regulatory protein 2 (ESRP2) in breast cancer and maternally expressed 3 (MEG3) in lung cancer[16].

CpG methylation, in addition to methylation-related genes, regulates cancer occurrence and development. DNA methylation is regulated by DNA methyltransferase (cytosine-5) 1 (DNMT1) in chronic myeloid leukemia and hepatocellular carcinoma[17,18]. The histone N-methyltransferase enzyme, enhancer of zeste homolog 2 (EZH2), is implicated in many important cancer types. Histone modification and histone deacetylase 1 (HDAC1) is also involved in the progression of breast cancer, pancreatic cancer and renal cell carcinoma[19], and HDAC inhibitors (HDACis) have obtained promising results in the clinic. Chidamide is a novel HDACi that has been used in lymphoma treatment[20,21]. However, the regulation of chidamide on BLACAT1 and miR-361expression in prostate cancer are poorly characterized.

Here, we have performed a range of experiments to dissect the role of BLACAT1 in prostate cancer progression and assess the potential roles of chidamide and 5-azacytidineas in cancer treatments.

## Patients and Methods

### Prostate Cancer Samples

Prostate cancer tumor tissue and healthy tissue were obtained from 25 patients treated at our local hospital between May 2015 and March 2016. Tissues were collected and stored at −80°C prior to experimental analysis. All patients completed informed consent forms and all study protocols were approved by the Institutional Ethical Committee of China Japan Union Hospital of Jilin University.

### Cell Culture

Human prostate cancer cell lines PC3 and DU145 cells and the normal prostate cell line RWPE-1 cells (Shanghai Hong Shun Biotechnology Co., Ltd., Shanghai, China) were cultured in complete Dulbecco's modified Eagle's medium (DMEM) (Invitrogen, Carlsbad, CA, USA) (supplemented with 10% fetal bovine serum (FBS) (Thermo Fisher Scientific, Waltham, MA, USA) and penicillin-streptomycin (Thermo Fisher Scientific, Waltham, MA, USA)) under standard culture conditions (37°C, 5% $CO_2$). For all experiments, cells ($5\times10^5$/well) were treated with predefined $EC_{50}$ of 5-azacytidine and chidamide.

### Lentiviral miR-361 Inhibitors and Mimics

Lentiviral vectors were used for all overexpression and/or depletion experiments. The BLACAT1 overexpression vector was synthesized by Invitrogen (Carlsbad, CA, USA). All miR-361 regents and clones were purchased from Invitrogen (Carlsbad, CA, USA). Lipofectamine 3000 (Carlsbad, CA, USA) was used for the transfection of LV-BLACAT1, LV-controls, miR-361 controls or miR-361 inhibitors.

### Cell Proliferation Assays

Transfected PC3 and DU145in 96-well plates (10000 cells/well) were treated with MTT (3-(4,5-dimethylthiazol-2-yl)-2,5-diphenyltetrazolium bromide) (10 µl) (Sigma-Aldrich, St. Louis, MO, USA) for 4 h. Absorbance values were read at 490 nm as per standard protocols as a measure of cell viability.

### Apoptosis Assays

To assess the number of apoptotic cells per sample, transfected cells were analyzed by flow cytometry after staining with Annexin V-FITC (fluorescein isothiocyanate) and propidium iodide (PI) (BD Biosciences, San Jose, CA, USA).

### Real-Time Polymerase Chain Reaction (RT-PCR) Analysis

For RT-PCR, total RNA was extracted via TRIzol lysis (Thermo Fisher Scientific, Waltham, MA, USA) and reverse transcription reactions were performed to produce cDNA at 42°C for 60 min; 25°C for 5 min; and 70°C for 5 min. The qPCR mixture (20 µl) consisted of 1 µl cDNA, 0.5 µl of each primer, 10 µl SYBR Green Mix (Invitrogen, Carlsbad, CA, USA), and 8 µl of diethyl pyrocarbonate (DEPC)-treated water. The qRT-PCR conditions: 95°C for 5 min; 45 x 95°C for 15

**Table I.** Primer sequences for RT-PCR.

| Gene | Primer | Product |
|---|---|---|
| BLACAT1 | Forward: 5'-CTCCCCTTCTAGCGCTCACG-3'<br>Reverse: 5'-CTAGCCGCCGTCTATACTACCGGCT-3' | 154 bp |
| DNMT1 | Forward: 5'-AGACACTCGCTCAGCTTCTTG-3'<br>Reverse: 5'-CAATTGCTGCTGGGATTCATC-3' | 106 bp |
| HDAC1 | Forward: 5'-CTGCTTTGTATTCCCTTTTGCA-3'<br>Reverse: 5'-TTGATTTCTCCTGGCTGTCTC-3' | 131 bp |
| EZH2 | Forward: 5'-CCTCCCGAGTGAAGTCATCGTGG-3'<br>Reverse: 5'-GGACAGGTGCTTCATCAGCTCG-3' | 142 bp |
| MDM2 | Forward: 5'-ACCACACGTTCCTAAGCTGG-3'<br>Reverse: 5'-TCCCTGCACGCAGAGATTTT-3' | 119 bp |
| Bax | Forward:5'-TCCCTGCACGCAGAGATTTT-3'<br>Reverse: 5'-TTGATTTCTCCTGGCTGTCTC-3' | 131bp |
| bcl-2 | Forward: 5'-AACCCTGCTGTTTGGCTTAAC-3'<br>Reverse: 5'-CGTACTTGCTGTACTCGCTCTTC-3' | 127 bp |
| ACTB | Forward: 5'-GAGCTACGAGCTGCCTGAC-3'<br>Reverse: 5'-GGTAGTTTCGTGGATGCCACAG-3' | 121 bp |

s; 60°C for 35 s; and 72°C for 20 s. The relative gene expression was calculated using the 2-ΔΔCT method (n = 3 reactions per sample). Primer sequences are shown in Table I.

### *miR-361 Expression*

RNeasy Mini Kit (Qiagen, Valencia, CA, USA) was used for total RNA extraction from both cell lines and tissues. qRT-PCR assays were performed using miScript Reverse Transcription kit (Qiagen, Valencia, CA, USA) and miScript SYBR® Green PCR kit (Qiagen, Valencia, CA, USA). PCR parameters: 95°C for 1 min; 40 x 95°C for 10 s; 55°C for 30 s; 70°C for 30 s. miRNA expression was normalized to U6 and calculated via the $2^{-\Delta\Delta CT}$ method.

### *Assessment of Methylation Status*

DNA isolation kit (Zymo, Irvine, CA, USA) was used for complementary DNA (cDNA) isolation. EZ DNA Methylation-Gold kit (Zymo, Irvine, CA, USA) was used to produce sulfated DNA, 2 µ of which was added with Zymo Taq PerMix (12.5 µl) (Zymo, Irvine, CA, USA), water (8.5 µl) and upstream and downstream primers (1 µl of each). PCR parameters: 95°C (10 min); 35 x 30 s at 95°C; 54°C (45 s); 72°C (45 s); extension at 72°C (7 min). Products were run on agarose gel (GoldView; Saibaisheng Bioengineering Co., Ltd., Beijing, China) in the following order: BLACAT1 methylated (M), BLACAT1 non-methylated (U) positive and negative methylation; BLACAT1 M and BLACAT1 U partially methylated; BLACAT1 M and BLACAT1 U positive and negative non-methylated. Table II lists all primer sequences.

### *Western Blotting*

Transfected cells were harvested in radio immunoprecipitation assay (RIPA) buffer, and proteins were resolved on 8-15% sodium dodecyl sulfate-polyacrylamide gel electrophoresis (SDS-PAGE) gels and transferred to polyvinylidene difluoride (PVDF) membrane (Amersham Pharmacia, Piscataway, NJ, USA). The PVDF membrane was washed in Tris-buffer saline (TBS), blocked with 5% skimmed milk in TBS, and was probed with anti-EZH2, anti-HDAC1, anti-MMP-2, anti-MMP-9, anti-Bax, anti-Bcl-2 and anti-ATCB primary antibodies (Abcam, Cambridge, MA, USA). Membranes were then washed and labeled

**Table II.** Primer sequences of the methylated BLACAT1 gene.

| Gene | Primer | Product |
|---|---|---|
| BLACAT1,M-MSP | Forward: 5'-CGTAGCTACTGCTATTATCGTTC-3'<br>Reverse: 5'-TTATGCCTTGGGCTACGTACT-3' | 162 bp |
| BLACAT1,U-MSP | Forward:5'-GGTACGTATGCTTGGGCTTATG-3'<br>Reverse: 5'-ATTGGCGCTTAGCTAGGCTA-3' | 162bp |

M, methylated; MSP, methylation-specific polymerase chain reaction; U, unmethylated.

with conjugated secondary antibodies. Protein bands were visualized on a BioSpectrum Imaging System (UVP, LLC, Upland, CA, USA).

### Luciferase Assays

LncRNA BLACAT1 (lncRNA-BLACAT1-wt) and its mutated 3'-untranslated region (3'-UTR) (lncRNA-BLACAT1-mu) were cloned into pRL-TK (Promega, Madison, WI, USA). Plasmids were co-transfected with miRNA mimics or negative control mimics and pGL3 as firefly luciferase control vector (Promega, Madison, WI, USA). Dual reporter assays were performed using the Promega system and assessed in a Modulus Single-tube Multimode Reader (Promega, Madison, WI, USA). pRL-TK values were normalized to pGL3. Assays were performed on a minimum of three independent occasions.

### RNA Pull-Down Assay

For the detection of KCNK15-AS1 binding proteins, Pierce Magnetic RNA-Protein Pull-Down Kit (Thermo Fisher Scientific, Waltham, MA, USA) was utilized. BLACAT1 lncRNAs (both sense and antisense) were synthesized and added to the PC3 cell lysates. The protein was then collected for mass spectrometry analysis.

### RNA Immunoprecipitations (RNA-IPs)

Magna RIP kit (EMD Millipore, Burlington, MA, USA) was used for RNA-IPs. Beads were resuspended, mixed with the samples at 4°C overnight. IPs products were washed for at least 6 times and RNA was extracted to determine its abundance.

### Chromatin Immunoprecipitation (ChIP)

Cells were crosslinked with formaldehyde and then harvested. Large DNA fragments (10-500 bp) were disrupted by sonification, and the HDAC1 and EZH2 antibodies/beads were added for protein-DNA precipitations. Cross-linking solution and sodium chloride were added at 65°C to dissociate the DNA and proteins. QIAGEN PCR kit (Qiagen, Hilden, Germany) was used for DNA and chromatin purifications and subsequent sequencing. Initial read outputs were filtered to remove potential contaminants and samples were sequenced to obtain clean data. Short oligonucleotide alignment program 2 (SOAP2) was employed to compare the reads with reference genomes according to each individual library read. Quality control (QC) assessments were performed to assess the quality of the sequencing according to known QC standards. All sequences were compared to the reference genome coverage and an in-depth statistical analysis of the genome loci was established. Furthermore, gene functional element distributions, gene enrichment and pathway enrichment analysis were performed.

### Xenograft Models

Athymic male mice (Chinese Academy of Science, Shanghai, China) were provided free access to water and food in laminar flow cabinets under pathogen-free conditions. To produce the models, stably transfected PC3 cells (control vector or LV-BLACAT1 expressing) were xenografted into BALB/c male nude mice. Each week, both the tumor volumes and weights were measured. After 35 d of tumor growth, tumors were collected from sacrificed mice for further analyses. The experiments involving animals were approved by The Animal Committee of Jilin university.

### Statistical Analysis

Data are expressed as the mean ± SD and analyzed using SPSS 19.0 (IBM Corporation, Armonk, NY, USA). Group data were compared using a one-way ANOVA (for multiple comparisons to the mean) or a Student's *t*-test for single group comparisons. A chi-squared test was used to compare rates. $p < 0.05$ indicated significant differences between groups.

## Results

### BLACAT1-Binding Proteins in PC3 Cells

Recent studies on lncRNA-binding proteins have established that the proteins that interact with lncRNAs regulate disease progression. RNA pull-downs were performed to reveal novel BLACAT1-binding proteins in PC3 cells, and the total number of BLACAT1-binding proteins was detected by mass spectrometry**.** The results showed that 1,823 unique proteins bound to BLACAT1. The results were first subjected to species selection; the polymorphic gene sequences were then compared with sequences in protein database. After choosing a homology higher than 99%, the results showed that EZH2, DNMT1 and HDAC1 interacted with BLACAT1.

### Increased Expression of DNA Modifying Genes and Proteins in Prostate Cancer Tissues

Following the results of the RNA pull-down results, the mRNA levels of BLACAT1, DNMT1,

HDAC1, EZH2, MDM2 and MIR361 were determined by using RT-PCR. BLACAT1 expression was significantly reduced in tumor *vs.* healthy tissue, while the gene expressions of DNMT1, HDAC1, EZH2, MDM2, and MIR361 were up-regulated in the tumor tissues (Figure 1A). Consistent with the gene expression data, DNMT1, HDAC1, EZH2 and MDM2 showed elevated levels of expression in cancer tissues *vs.* adjacent non-cancerous tissues (Figures 1B-C).

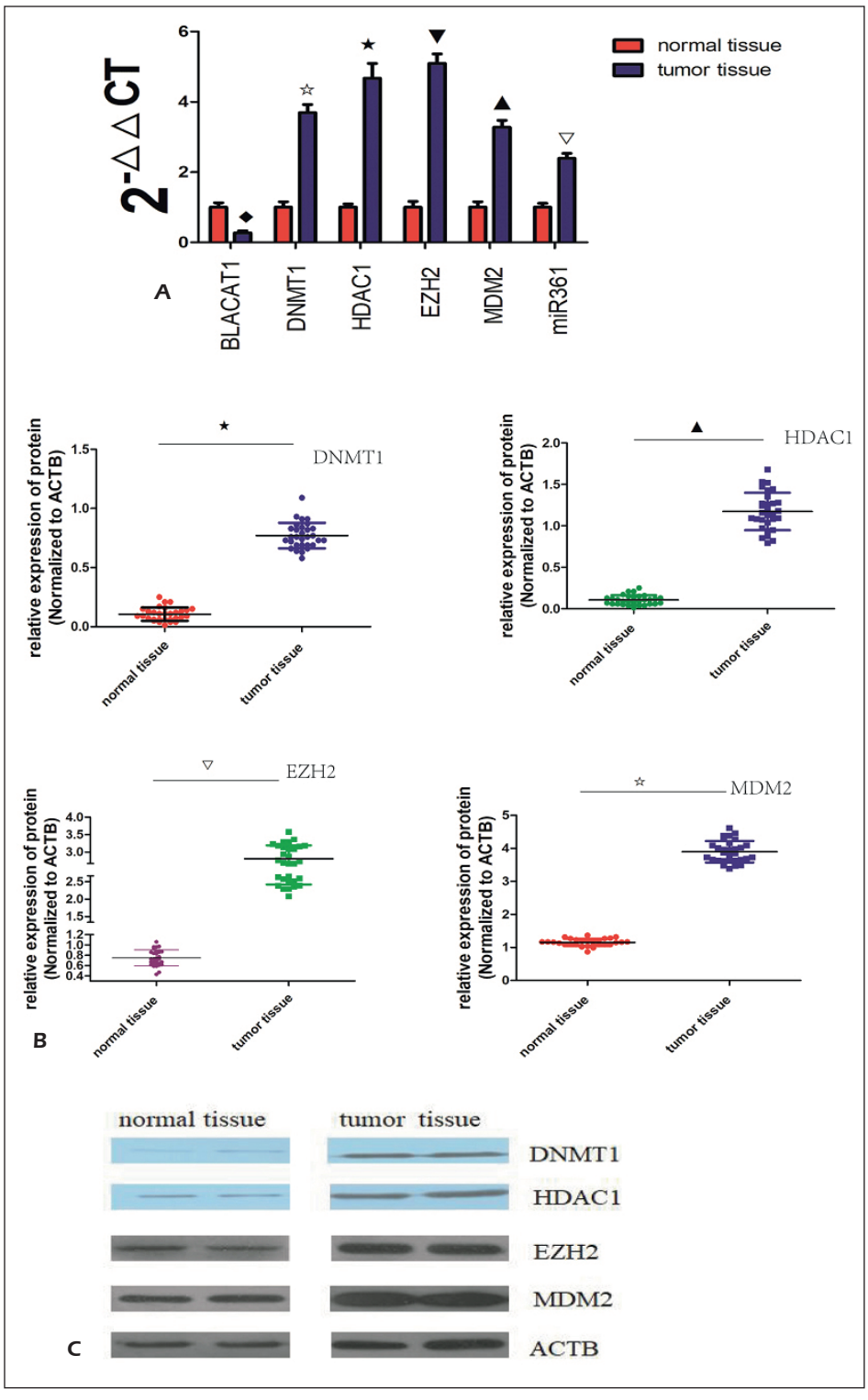


**Figure 1.** mRNA expression in normal and tumor tissue determined by RT-qPCR. **A**, mRNA expressions of BLACAT1, DNMT1, HDAC1, EZH2, MDM2, and MIR-361 in tumor tissue *vs.* normal tissue (◇☆★▼▲▽$p<0.05$). **B**, Protein levels of the genes in both tissues (★▲▽☆, $p<0.05$). **C**, β-actin was probed as a loading control.

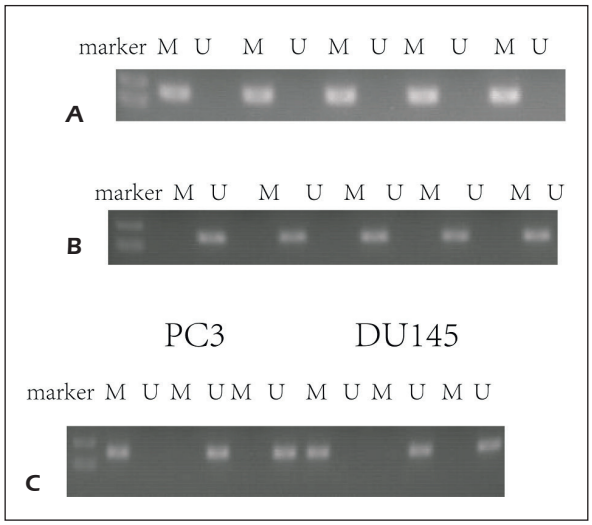


**Figure 2.** Methylation status of BLACAT1 determined by MSP. **A**, BLACAT1 was methylated in tumor tissue. **B**, BLACAT1 was non-methylated in normal tissue. **C**, BLACAT1 was methylated in both prostate cancer cell lines but became non-methylated following drug treatment.

### The BLACAT1 Promoter is Methylated in Prostate Cancer

Methylation-specific PCR (MSP) was performed on the BLACAT1 promoter in prostate cancer tissue *vs.* adjacent non-cancerous tissue. Prostate tumor tissues showed that the levels of BLACAT1 promoter methylation (Figure 2A) were high in tumor tissue and absent in adjacent non-cancerous tissues. *BLACAT1* promoter methylation was confirmed *in vitro* in the prostate cancer cell lines. Following treatment with chidamide and 5-azacytidine, BLACAT1 methylation was absent (Figure 2C).

### Chidamide and 5-Azacytidine Inhibit the Expression of DNA Modifying Genes

We next assessed epigenetic regulation in the presence of chidamide and 5-azacytidine. In the experiments that followed, PC3 and DU145 cells were exposed to a range of concentrations of each compound in which BLACAT1 mRNA expression increased, while the expression of DNMT1, HDAC1, EZH2, MDM2, and MIR361 decreased (Figures 3A-B). These effects on gene expression were confirmed by Western blot assessments of protein expression (Figures 3C-D).

### BLACAT1 Overexpression Slows Cells Growth and Leads to Apoptotic Induction

BLACAT1 mRNA expression was initially assessed in PC3, DU145 and RWPE-1 cells. BLACAT1 mRNA expression was lower in PC3/DU145 cells *vs.* RWPE-1 cells **(Supplementary Figure 1A)**. LV-BLACAT1 was then transfected into PC3 and DU145 cells, and increased BLACAT1 levels were verified by RT-PCR **(Supplementary Figure 1B).** We next performed MTT viability assays to assess the influence of BLACAT1 on cell growth and apoptosis. Transfection with BLACAT1 slowed the growth of both prostate cancer cell lines at 72 h and 96 h, respectively (Figure 4A). *In vivo* assessments showed that the overexpression of *BLACAT1* slowed tumor growth at 28 days and 35 days (Figure 5). We performed Annexin-PI staining to determine the influence of BLACAT1 on PC3 and DU145cell apoptosis. BLACAT1 overexpression led to apoptotic induction in both cell lines (Figure 4B). We further analyzed the expression of apoptotic associated proteins including Bcl-2, Bax, matrix metallopeptidase 2 (MMP-2), and matrix metallopeptidase 9 (MMP-9) following the exogenous expression of BLACAT. The results showed that high BLACAT1 levels suppressed Bcl-2, MMP-2, and MMP-9, but increased Bax expression in PC3 and DU145 cells, underliying the roles of these proteins in the BLACAT mediated effects on prostate cancer cell survival (Figures 4C-D).

### BLACAT1 Interacts with miR-361

CeRNAs are lncRNAs that produce a sponge effect through their binding to miRNAs that block their subsequent effects on gene expression. We investigated if BLACAT1 acts via this mechanism through luciferase reporter assay, which assessed the binding of BLACAT1 to miR-361. The relative luciferase activity showed no differences between miR-361 control and mimics groups after the transfection of the mutant 3'-UTR of BLACAT1. However, luciferase activity declined in the miR-361 mimic groups compared to miR-361 control group after transfection of wild 3'-UTR of BLACAT1 (Figure 6A**)**. Using the RNA up algorithm, significant complementary regions were predicted, suggesting that miR-361 binds to BLACAT1 (Figure 6B**)**. RIP results showed that the fold enrichment of lncRNA BLACAT1 was elevated in EZH2 and MDM2 groups *vs.* the IgG alone group (Figure 5C). Furthermore, the overexpression of BLACAT1 led to a loss of miR-361 in both PC3 and DU145 prostate cancer cells (Figures 6D-E).

### Knockdown of miR-361 Slows Prostate Cancer Growth and Promotes Cell Death

To reveal the effects of miR-361 in prostate cancer cells, its expression was detected in PC3

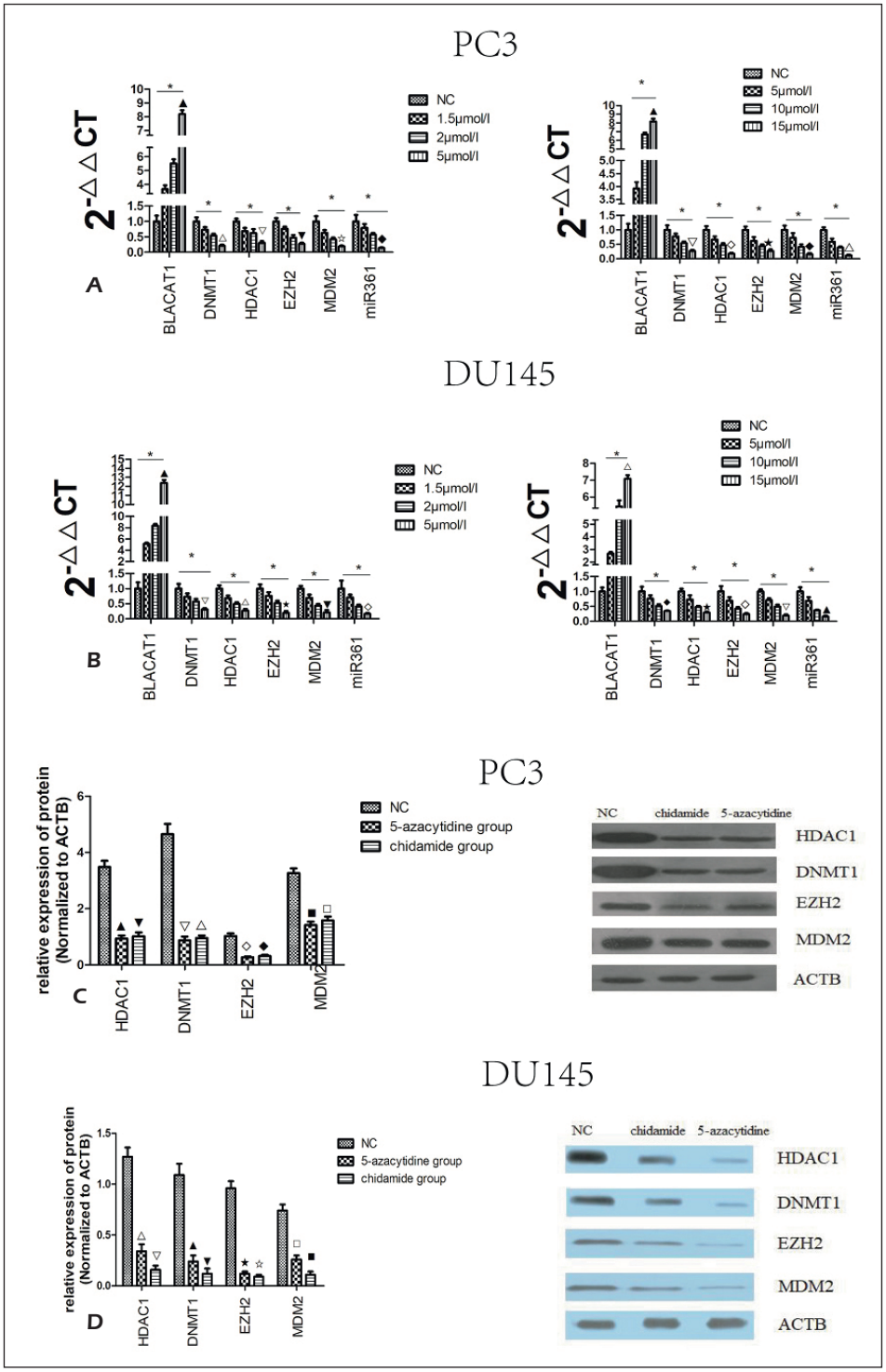


**Figure 3.** Gene and protein expressions following treatment with chidamide or 5'azacytidine. **A**, mRNA expressions of BLACAT1, DNMT1, HDAC1, EZH2, MDM2 and MIR361 following drug treatment in PC3 cells (▲△▽▼☆◆, $p<0.05$). **B**, mRNA levels of the aforementioned genes following drug treatments in DU145 cells (▲▽◇★◆△, $p<0.05$). **C**, DNMT1, HDAC1, EZH2 and MDM2 expressions at the protein level following 5-azacytidine orchidamide treatment in PC3 cells (▲▼▽△◇◆■□, $p<0.05$). β-actin was probed as a loading control. **D**, Expressions of DNMT1, HDAC1, EZH2 and MDM2 at the protein level following 5-azacytidine or chidamide treatment in DU145 cells (▽△▲▼★☆■□, $p<0.05$).

and DU145, and found to be significantly higher than that of RWPE-1 cells **(Supplementary Figure 1A)**. To further analyze the roles of miR-361, miR-361 inhibitors were transfected into PC3 and DU145 cells **(Supplementary Figure 1C)** and cell viability and proliferation were assessed via MTT assays. The inhibition of miR-361 expression caused a delayed cell growth 72 h post-transfection (Figure 7A). We further performed flow cytometry to investigate the effects of miR-361 on

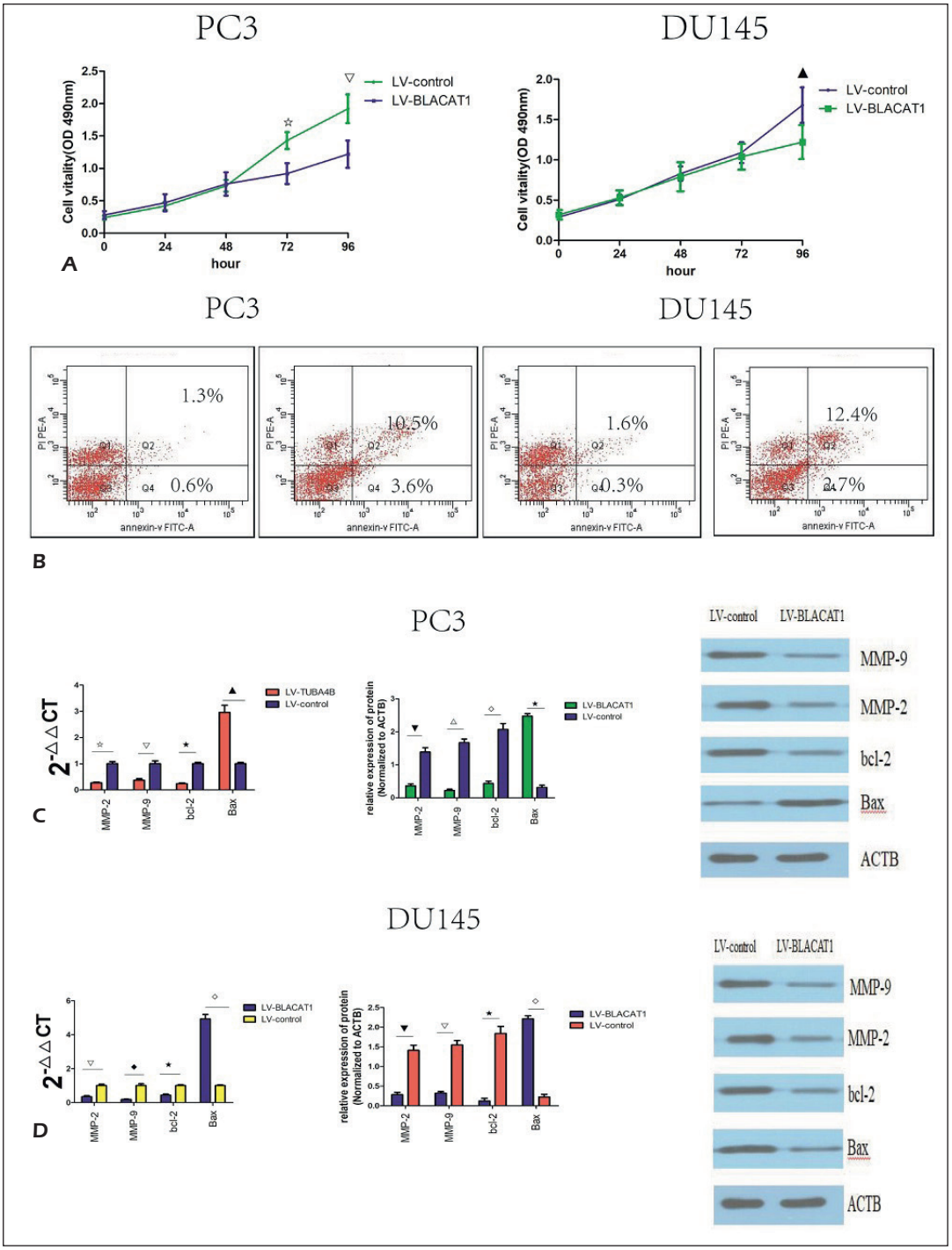


**Figure 4.** **A**, PC3 and DU145 proliferation assays following the overexpression of BLACAT1 (☆▽▲, $p<0.05$). **B**, Apoptosis assessments in cells overexpressing BLACAT1. **C**, MMP2, MMP-9, Bax, and Bcl-2 expressions in PC3 cells following BLACAT1 overexpression (☆▽★▲▼△◇★, $p<0.05$). **D**, MMP2, MMP-9, Bax, and Bcl-2 expressions in DU145 cells following BLACAT1 overexpression (▽◆★◇▼▽★◇, $p<0.05$).

PC3 and DU145 cell apoptosis. MiR-361 silencing enhanced the apoptotic rates of both prostate cancer cell lines (Figure 7B). These effects were confirmed through the expressions of Bcl-2, Bax, MMP-2 and MMP-9. MiR-361 silencing led to a loss of Bcl-2, MMP-2 and MMP-9 expressions at both the mRNA and protein levels, while Bax expression was enhanced (Figures 7C-D).

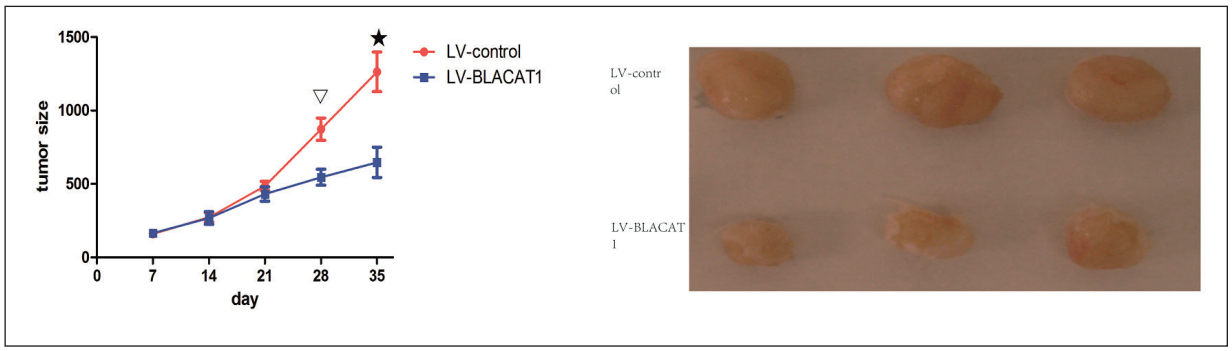


**Figure 5.** Tumor sizes in BLACAT1 overexpression groups *vs.* the control group (▼☆$p$<0.05).

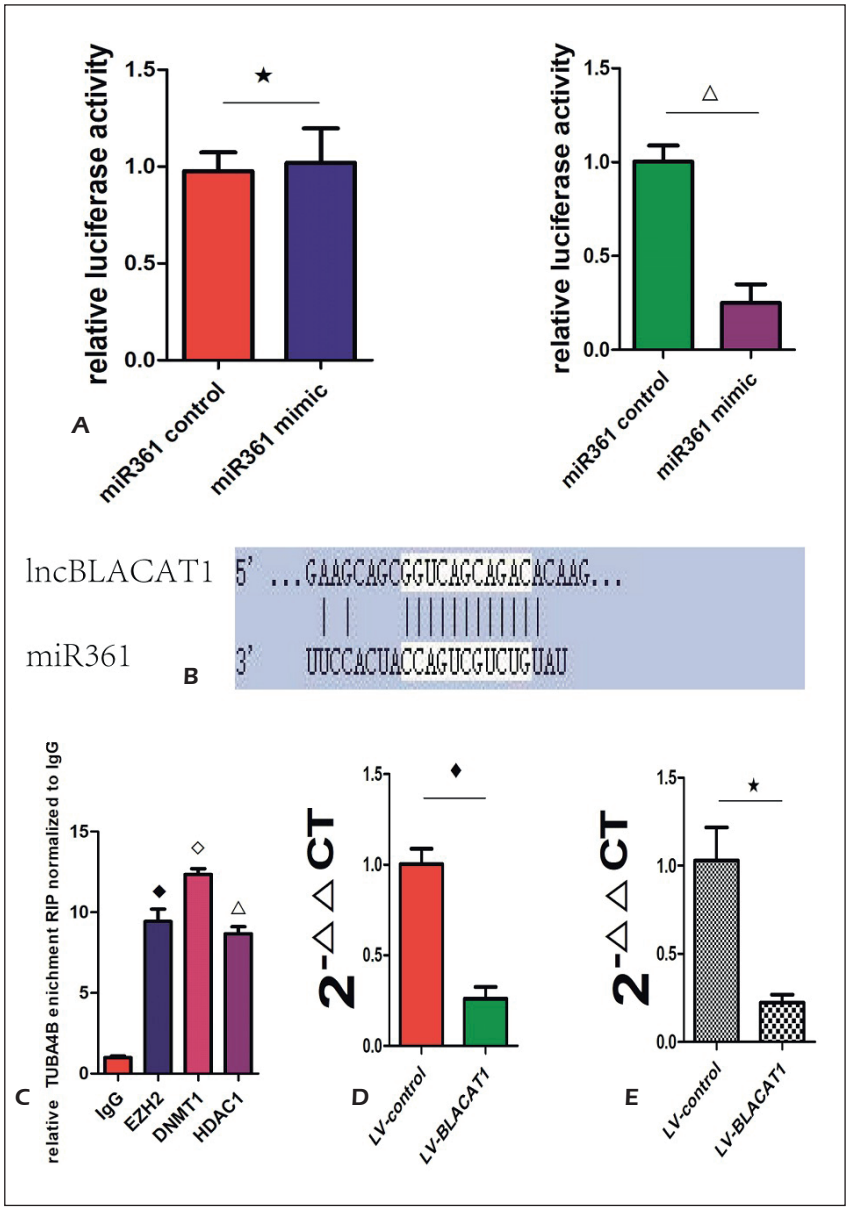


**Figure 6.** **A**, miR-361 mimics and the miR-361 control groups after transfection of mutant or wild 3'-UTR of BLACAT1. **B**, miR-361 binds to BLACAT1 through complementary sequences in the indicated regions, as predicted by the RNA up algorithm **C**, Fold enrichment of lncRNA BLACAT1 was elevated in EZH2 and MDM2 groups *vs.* the IgG group. **D**, miR-361 expression following BLACAT1 overexpression in PC3 cells. **E**. miR-361 expression following BLACAT1 overexpression in DU145 cells.

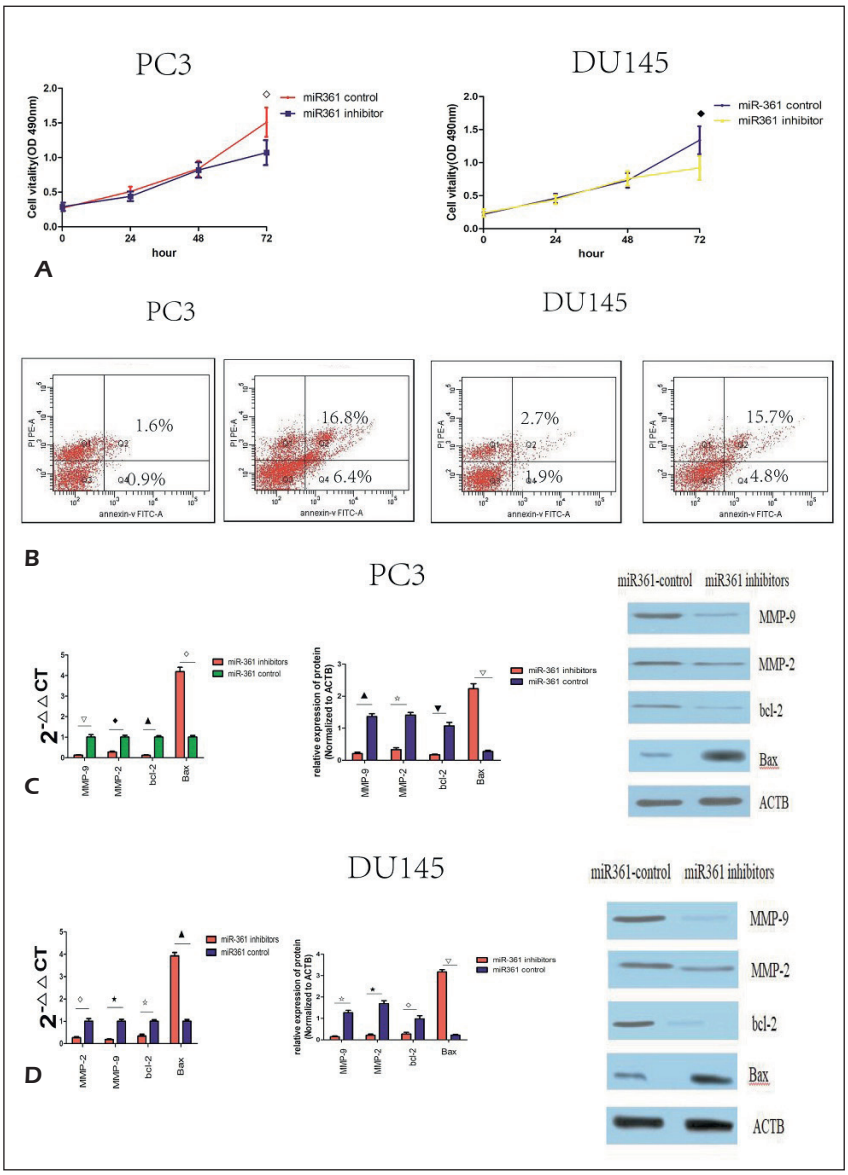


**Figure 7. A**, PC3 and DU145 cell proliferation assay following miR-361 inhibition (◇△$p$<0.05). **B**, Apoptosis assessment in the prostate cancer cell lines following miR-361 inhibition. **C**, MMP2, MMP-9, Bax and Bcl-2 expressions following miR-361 inhibition in PC3 cells (▽◆▲◇▲☆▼▽, $p$<0.05). **D**, MMP2, MMP-9, Bax and Bcl-2expressions following miR-361 inhibition in DU145 cells (◇★☆▲P☆★◇▽, $p$<0.05).

### *EZH2 and HDAC1 Interacting Partners*

Following sequencing, we identified 26,347,096 original reads which. After filtering, it was revealed that the mitogen-activated protein kinase (MAPK) can interact with EZH2. After sequencing, 69,837,024 original reads were obtained. Upon filtering, it was revealed that HDAC1 interacted with the STAT3 promoter region.

## Discussion

Prostate cancer remains a leading cause of death across the globe, most commonly in elderly males. To-date, prostate cancer diagnostics are lacking due to the lack of early symptoms during disease progression. Despite the intense research efforts, the mechanisms of prostate cancer development remain poorly understood and effective chemotherapeutic treatment regimens are lacking. To improve prostate cancer therapies, a clear understanding of the main cancer drivers is required.

Here, we have identified two regulatory axes namely BLACAT1-EZH2-MAPK and BLACAT1-HDAC1-STAT3 that are associated with prostate cancer progression. MiR-361, the target miRNA of BLACAT1, was additionally detected to be associated with prostate cancer progression due to its effects on PC3 and DU145 cell lines. Chidamide and 5-azacytidine were further revealed as promising prospects for prostate cancer treatment.

Consistent with the literature, we found that BLACAT1 is downregulated in prostate cancer tissue due to its methylation confirmed by MSP. This highlighted the high methylation rates of BLACAT1 as a potentially key event during breast cancer prognosis.

Histone deacetylation and DNA methylation both influence promoter activity and subsequent gene expression[14,22,23]. CpG island methylation is strongly regulated by members of the DNA methyltransferase (DNMT) family including DNMT1[24], while histone modifications are regulated by the HDAC family[25]. The expressions of DNMT1, HDAC1, MDM2 and EZH2 were at high levels in prostate cancer tissue. It was therefore speculated that DNMT1, HDAC1, MDM2 and EZH2 could act as key regulators of prostate cancer development.

Exposing *in vitro* prostate cancer lines to chidamide and 5-azacytidine led to enhanced levels of BLACAT1. This phenomenon revealed that BLACAT1 expression mediates histone acetylation in addition to DNA methylation.

We further revealed that miR-361 is a cellular target for BLACAT1. BLACAT1 overexpression and miR-361 silencing reduced cell growth and enhanced the apoptotic rates of prostate cancer cells. Further analysis of the expression of key mediators of cellular apoptotic pathways revealed that these effects were mediated by a loss of Bcl-2 expression and increased levels of Bax. Thus, both BLACAT1 overexpression and miR-361 silencing slowed cell cycle progression and promoted apoptotic cell death through downregulating the expression of Bcl-2 in prostate cancer cells. The overexpression of both MMP-2 and MMP-9 have been implicated in an array of lethal human cancers including cervical, ovarian, hepatocellular, head, neck and thyroid carcinomas, in addition to squamous cell carcinomas[26,27]. In this study, BLACAT1 overexpression and miR-361 silencing led to a loss of these oncogenic proteins in prostate cancer cells, revealing new insights into the roles of these host factors in the progression and development of prostate cancer. Furthermore, RNA pulldown and RIP analysis showed that DNMT1, EZH2 and HDAC1 interacted with BLACAT1, suggesting that these proteins regulate BLACAT1 expression. ChIP-seq was performed to detect HADC1 and EZH2 expressions in prostate cancer cells, which revealed that EZH2 interacted with the MAPK promoter while HDAC1 interacted with the promoter of STAT3. It was therefore speculated that MAPK regulates EZH2 while STAT3 regulates HDAC1, implicating a role for both genes in the regulation of BLACAT1.

## Conclusions

We identified two regulatory axes of BLACAT1-EZH2-MAPK and BLACAT1-HDAC1-STAT5, which were associated with prostate cancer progression. Chidamide and 5-azacytidine might provide new ideas in treating prostate cancer.

### Authors' Contributions

Hong-yan Li, Fu-quan Jiang and Lin Chu carried out the experiments and Xin Wei prepared the manuscript.

### Conflict of Interests

The Authors declare that they have no conflict of interests.

## References


1) Kim HL, Halabi S, Li P, Mayhew G, Simko J, Nixon AB, Small EJ, Rini B, Morris MJ, Taplin ME, George D. A molecular model for predicting overall survival in patients with metastatic clear cell renal carcinoma: results from CALGB 90206 (Alliance). EBioMedicine 2015; 2: 1814-1820.
2) Zhang D, Tang DG. "Splice" a way towards neuroendocrine prostate cancer. EBioMedicine 2018; 35: 12-13.
3) Munkley J, Vodak D, Livermore KE, James K, Wilson BT, Knight B, Mccullagh P, Mcgrath J, Crundwell M, Harries LW, Leung HY, Robson CN, Mills IG, Rajan P, Elliott DJ. Glycosylation is an androgen-regulated process essential for prostate cancer cell viability. EBioMedicine 2016; 8: 103-116.
4) Lee AR, Gan Y, Tang Y, Dong X. A novel mechanism of SRRM4 in promoting neuroendocrine prostate cancer development via a pluripotency gene network. EBioMedicine 2018; 35: 167-177.
5) Wang L, Wang J, Xiong H, Wu F, Lan T, Zhang Y, Guo X, Wang H, Saleem M, Jiang C, Lu J, Deng Y. Co-targeting hexokinase 2-mediated Warburg effect and ULK1-dependent autophagy suppresses tumor growth of PTEN- and TP53-deficiency-driven castration-resistant prostate cancer. EBioMedicine 2016; 7: 50-61.
6) Munschauer M, Nguyen CT, Sirokman K, Hartigan CR, Hogstrom L, Engreitz JM, Ulirsch JC, Fulco CP, Subramanian V, Chen J, Schenone M, Guttman M, Carr SA, Lander ES. The NORAD lncRNA assembles a topoisomerase complex critical for genome stability. Nature 2018; 561: 132-136.
7) Luo Z, Rhie SK, Lay FD, Farnham PJ. A prostate cancer risk element functions as a repressive loop that regulates HOXA13. Cell Rep 2017; 21: 1411-1417.
8) Zhang Y, Zhang P, Wan X, Su X, Kong Z, Zhai Q, Xiang X, Li L, Li Y. Downregulation of long non-coding RNA HCG11 predicts a poor prognosis in prostate cancer. Biomed Pharmacother 2016; 83: 936-941.

9) Xu W, Chang J, Du X, Hou J. Long non-coding RNA PCAT-1 contributes to tumorigenesis by regulating FSCN1 via miR-145-5p in prostate cancer. Biomed Pharmacother 2017; 95: 1112-1118.
10) He W, Cai Q, Sun F, Zhong G, Wang P, Liu H, Luo J, Yu H, Huang J, Lin T. linc-UBC1 physically associates with polycomb repressive complex 2 (PRC2) and acts as a negative prognostic factor for lymph node metastasis and survival inbladder cancer. Biochim Biophys Acta 2013; 1832: 1528-1537.
11) Chen W, Hang Y, Xu W, Wu J, Chen L, Chen J, Mao Y, Song J, Song J, AUID- Oho, Wang H. BLACAT1 predicts poor prognosis and serves as oncogenic lncRNA in small-cell lung cancer. J Cell Biochem 2019; 120: 2540-2546.
12) Su J, Zhang E, Han L, Yin D, Liu Z, He X, Zhang Y, Lin F, Lin Q, Mao P, Mao W, Shen D. Long non-coding RNA BLACAT1 indicates a poor prognosis of colorectal cancer and affects cell proliferation by epigenetically silencing of p15. Cell Death Dis 2017; 8: e2665.
13) Fuentes-Mattei E, Giza DE, Shimizu M, Ivan C, Manning JT, Tudor S, Ciccone M, Kargin OA, Zhang X, Mur P, do ANS, Chen M, Tarrand JJ, Lupu F, Ferrajoli A, Keating MJ, Vasilescu C, Yeung SJ, Calin GA. Plasma viral miRNAs indicate a high prevalence of occult viral infections. EBioMedicine 2017; 20: 182-192.
14) Herman JG, Baylin SB. Gene silencing in cancer in association with promoter hypermethylation. N Engl J Med 2003; 349: 2042-2054.
15) Ye M, Huang T, Ni C, Yang P, Chen S. Diagnostic capacity of RASSF1A promoter methylation as a biomarker in tissue, brushing, and blood samples of nasopharyngeal carcinoma. EBioMedicine 2017; 18: 32-40.
16) Sun L, Li Y, Yang B. Downregulated long non-coding RNA MEG3 in breast cancer regulates proliferation, migration and invasion by depending on p53's transcriptional activity. Biochem Biophys Res Commun 2016; 478: 323-329.
17) Barcena-Varela M, Caruso S, Llerena S, Alvarez-Sola G, Uriarte I, Latasa MU, Urtasun R, Rebouissou S, Alvarez L, Jimenez M, Santamaria E, Rodriguez-Ortigosa C, Mazza G, Rombouts K, Jose-Eneriz ES, Rabal O, Agirre X, Iraburu M, Santos-Laso A, Banales JM, Zucman-Rossi J, Prosper F, Oyarzabal J, Berasain C, Avila MA, Fernandez-Barrena MG. Dual targeting of histone methyltransferase G9a and DNA-methyltransferase 1 for the treatment of experimental hepatocellular carcinoma. Hepatology 2019; 69: 587-603.
18) Wang Q, Wang Y, Xing Y, Yan Y, Guo P, Zhuang J, Qin F, Zhang J. Physcion 8-O-beta-glucopyranoside induces apoptosis, suppresses invasion and inhibits epithelial to mesenchymal transition of hepatocellular carcinoma HepG2 cells. Biomed Pharmacother 2016; 83: 372-380.
19) Huang Z, Zhou W, Li Y, Cao M, Wang T, Ma Y, Guo Q, Wang X, Zhang C, Zhang C, Shen W, Liu Y, Chen Y, Zheng J, Yang S, Fan Y, Xiang R. Novel hybrid molecule overcomes the limited response of solid tumours to HDAC inhibitors via suppressing JAK1-STAT3-BCL2 signalling. Theranostics 2018; 8: 4995-5011.
20) He J, Chen Q, Gu H, Chen J, Zhang E, Guo X, Huang X, Yan H, He D, Yang Y, Zhao Y, Wang G, He H, Yi Q, Cai Z. Therapeutic effects of the novel subtype-selective histone deacetylase inhibitor chidamide on myeloma-associated bone disease. Haematologica 2018; 103: 1369-1379.
21) Mao J, Li S, Zhao H, Zhu Y, Hong M, Zhu H, Qian S, Li J. Effects of chidamide and its combination with decitabine on proliferation and apoptosis of leukemia cell lines. Am J Transl Res 2018; 10: 2567-2578.
22) Chen YL, Zhang ZX, Shou LH, Di JY. Regulation of DNA methylation and tumor suppression gene expression by miR-29b in leukemia patients and related mechanisms. Eur Rev Med Pharmacol Sci 2018; 22: 158-165.
23) Huang J, Ding CH, Li ZY, Zhang XB, You ZS, Zhou CQ, Xu YW. Epigenetic changes of histone deacetylation in murine oocytes matured in vitro versus *in vivo*. Eur Rev Med Pharmacol Sci 2017; 21: 2039-2044.
24) Lyko F. The DNA methyltransferase family: a versatile toolkit for epigenetic regulation. Nat Rev Genet 2018; 19: 81-92.
25) Riccio A. New endogenous regulators of class I histone deacetylases. Sci Signal 2010; 3: pe1.
26) Zhang Y, Ni HJ, Zhou HS. Study on the expression of Toll-like receptor 4 and matrix metalloproteinase-9 in patients with chronic obstructive pulmonary disease and their clinical significance. Eur Rev Med Pharmacol Sci 2017; 21: 2185-2191.
27) Turgut A, Goruk NY, Tunc SY, Agaçayak E, Alabalik U, Yalinkaya A, Gül T. Expression of extracellular matrix metalloproteinase inducer (EMMPRIN) in the endometrium of patients with repeated implantation failure after in vitro fertilization. Eur Rev Med Pharmacol Sci 2014; 18: 275-280.